Analytical and Numerical Methods in Mechanical Design
Vol.1, Issue 2, Summer & Autumn 2022, 23-37

Free Vibration Analysis of Sandwich Plates with FGM Face Sheets and Temperature-Dependent Properties of the Core Materials

Y. Mohammadi [1,*]

[1] *Faculty of Industrial and Mechanical Engineering, Islamic Azad University, Qazvin Branch, Qazvin, Iran*
Received: 21 July 2022- Accepted: 03 September 2022
*Corresponding author: *u.mohammadi@gmail.com*

Abstract

In this paper, the free vibration of sandwich plates with power-law FGM face sheets in various thermal environments is performed by high-order sandwich plate theory. The material properties of the core, such as Young’s modulus, density, thermal expansion coefficient and Poisson’s ratio, are assumed to be temperature dependent by nonlinear function of temperature [1]. The material properties of the FGM face sheets are assumed to vary continuously through the thickness according to a power law distribution in terms of volume fractions of the constituents [2]. The governing equations of motion in free natural vibration are derived using Hamilton’s principle [3]. A new approach is used to reduce the equations of motion from twenty three equations to eleven equations and then solve them. The new solution approach consists of isolating six of the unknowns in the displacements of the face sheets using the compatibility equations, followed by isolating the additional six Lagrange multipliers using the equations of the face sheets, finally, the isolated unknowns are substituted into the eleven equations of the core. Both un-symmetric and symmetric sandwich plates are considered in this analysis. Good agreement is found between theoretical predictions of the fundamental frequency parameters and the results obtained from other references for simply supported sandwich plates with functionally graded face sheets. The results show that the fundamental frequency parameters (ω □) increases by increasing the volume fraction index (κ). Also, the effect of temperature on the value of fundamental frequency parameters decreases with increases in the FGM face sheets thickness. The results also revealed that as the side-to-thickness ratio (b⁄h), the core-to-face sheet thickness ratio (h_c⁄h_t) and temperature changes, have a significant effect on the fundamental frequency parameters.

***Keywords*:** Sandwich Plates; FGM; Free Vibration; Temperature Properties

1. Introduction

A typical advanced construction of a sandwich plate consists of two FGM face sheets, not necessarily identical, bonded to the compressible core through adhesive layers. The separation of FGM face sheets by a soft core increases the bending rigidity of the plate at a expenses of small weight. Also, the functionally graded materials (FGMs) are multi-functional materials which contain spatial variations in composition and microstructure for the specific purpose of controlling variations in thermal, structural or functional properties. These materials are presently in the forefront of material research receiving worldwide attention [1]. Such materials have a broad range of applications including for example, biomechanical, automotive, aerospace, mechanical, civil, nuclear, and naval engineering. FGMs are microscopically inhomogeneous composites usually made from a mixture of metals and ceramics. The considerable advantages offered by FGMs over conventional materials and the need of overcoming the technical challenges involving high temperature environments have prompted an increased use of sandwich structures, and incorporation in their construction are the FGMs as face sheets [1,2].
The classical linear and non-linear analytical approaches, see for example Allen [3], Plantema [4], Zenkert [5], Vinson [6] and some recent comprehensive reviews, Noor [7] and Librescue [8], emphasize on traditional sandwich panels, made of metallic, anti-plane, incompressible honeycomb cores and fully bonded face-core interfaces. These models assumed that the face sheets have only bending rigidity, while the core has only shear rigidity. For the prediction of the overall load response of sandwich plates subjected to bending, shear and buckling loads, as well as undergoing free or forced vibrations, most analyses adopt the so-called “equivalent single layer” approach based on the first-order shear deformable model, see Mindlin [9], or based on a high-order approach, see Reddy [10]. Most of the aforementioned models ignore the effects of the transversely flexible core, such as changes of the height of the sandwich plate, non-linearity of the section plane after

deformation, and different boundary conditions at the upper and the lower face sheets.

Recently, Carrera and Demasi [11], Carrera and Ciuffreda [12] and Carrea [13] have presented ESL and layer-wise models with various plate theories for the analysis of sandwich panels with and without vertical normal strain. The classical and the ESL models, in general, usually disregard the changes in the height of the core (i.e. the vertical compressibility) when the panel is deformed. Hence, when using these approaches, for the free vibration response, the throughthickness modes of the core cannot be detected. Examples of research works following these approaches include Kant and Mallikarjuna [14] and Kant and Swaminathan [15] who used a highorder model but with an incompressible core, and Meunier and Shenoi [16], Bardell et al. [17] and Lee and Fan [18] who used different finite elements analysis approaches adopting various pre-assumed displacement distributions.

An extensive literature search reveals that only a limited number of research works are available in open literature that take into account the temperature-dependent both face sheets and core material properties in their analyses.

Moreover, the available research works are based on the assumption of an incompressible core, and they adopt the equivalent single layer (SL) approach along with various finite element analysis formulations. Examples of such research works include Vangipuram and Ganesan [19] who assumed a viscoelastic core and used a finite element formulation, Shiau and Kuo [20], who used the splitted rigidity approach (Allen [3] and Plantema [4], Ibrahim [21]) to discuss the case of a sandwich panel made of a functionally graded material (FGM), Kim [22] dealt with an FGM panel, Hao and Rao [23] assumed a core made of a pressure sensitive adhesive (PSA), and Duan et al. [24] dealt with a sandwich panel utilizing shape memory alloys (SMA) at elevated temperatures. Generally, the classical sandwich theories, based on the ESL and high-order models, mentioned above, are unable to detect the high-order modes that are associated with deformations through the thickness of the core. Because they ignore vertical compressibility of the core, or in the other words the changes in the height of the core, during the deformation of the sandwich structure.

The non-planar deformed cross-section of the sandwich plate, observed experimentally by Petras and Sutcliffe [25], suggested the need for a model which allows non-linear variations of in-plane and vertical displacement field through the core. Frostig and Baruch [26,27] used variational principles to develop a high-order sandwich panel theory, which includes the transverse flexibility of the core. In contrast, the simple beam theory where the core in-plane displacements are assumed to vary in a linear way through the depth, and the out-of-plane displacements are assumed to be constant. The High-Order Sandwich Panel Theory (HSAPT) model takes into account the effects of the vertical flexibility of the core and its shear resistance on the linear and the non-linear responses, see Frostig et al. [26] for the general linear response, see Frostig and Baruch [28] and Frostig [29] for the non-linear response due to inplane compressive loading of unidirectional sandwich structures, and Sokolinsky and Frostig [30–32] for the non-linear response of various sandwich beams and panels.

This theory has been successfully used by the authors and for the analysis of various linear and non-linear applications, such as, Frostig and Baruch [33] for high-order vibration of sandwich panels; Bozhevolnaya and Frostig [34] dealt with the vibration of curved sandwich panels; Frostig and Thomsen [35] treated the vibration of sandwich plates; Yang and Qiao [36] and Qiao and Yang [37] used the HSAPT model and its modification for impact problems; Schwarts-Givli et al. [38–41] dealt with free and forced vibrations of delaminated sandwich panels; Malekzadeh, Khalili and Mittal [42] analysis the local and global damped vibrations of sandwich plates by an improved HSAPT; and recently Frostig and Thomsen [43r,44] treated the non-linear response of sandwich panel with temperature-dependent properties. But in use of HSAPT model, they always disregarded the in-plane stresses of the core. Because, the core of their sandwich structures has only out of plane resistance.

The improved model used in present paper considers the both in-plane and out of plane resistances of the core and assumes that the distribution of the in-plane and vertical core displacements can be represented as cubic and quadratic polynomials, respectively [45]. The variational principle of minimum of the total potential energy is used to derive the field equations along with the appropriate boundary conditions. The unknowns in this model consist of the displacements of the face sheets and the coefficients of the polynomials in the core. In this formulation, the effects of the non-uniform stiffness of the core are implemented following a straight forward approach. Here, the high-order stress resultants of the non-uniform core are determined using a direct integration process, and because the core in-plane stresses considered in this improved model, we have twelve in-plane high-order stress resultants, as well as, eight out of plane high-order stress resultants. It should be noticed that this improved model involves higher-order core stress resultants that have no physical interpretation, and the model yields higher-order modes that involve vibrations through the depth of the core that the HSAPT model cannot detect. So, "displacements formulation" model extended to the case of free vibration of sandwich plates with power-law FGM face sheets and temperature dependent both the core and the face sheets material properties with considering the core in-plane stresses in this paper. Also, it should be noticed that both un-symmetric and symmetric sandwich plates are considered in here.

Since FGMs are used in high-temperature environments, the constituents of FGM face sheets possess temperature-dependent properties. Therefore, the material properties of the FGM face sheets must be temperature dependent and position dependent. When the material properties are assumed to be functions of temperature and position, and the temperature is also assumed to be a function of position, the problem becomes very complicated.

Another novel contribution of the present work is use of the new approach to reduce the equations of motion from twenty three equations that are functions of core constants, face sheets constants and Lagrange constants to eleven equations that are just functions of eleven core constants, this approach illustrated clearly in section 3. The material properties of FGM face sheets are assumed to be graded in the thickness direction according to a simple power-law distribution in terms of the volume fractions of the constituents, and the material properties of both FGM face sheets and the homogeneous core are assumed to be temperature dependent by a third order function of temperature.

The numerical results show the effect of temperature changes, volume fraction distribution of FGM face sheets, side-to-thickness ratio and core-to-face sheet thickness ratio on the free vibration characteristics of defined sandwich plate.

2.Formulation

The displacement formulation (model II) of Frostig and Thomsen [45] is improved and then is used in this paper. The equations of motions of the free vibration response are derived through the Hamilton principle which extremizes the Lagragian that consists of the kinetic and the internal potential energy as follows:

$$\int_{t_1}^{t_2}(\delta T+\delta U)\,dt=0 \qquad (1)$$

Where T and U are kinetic energy and internal potential energy, respectively; t is the time coordinate that varies between the times $t_1$and t_2; and δ denotes the variation operator.

Consider a sandwich plate of length a and width b, consisting of a core with thickness h_c, Young's and shear modulus $E_c$and G_c, respectively, and two FGM face sheets with the thicknesses of $h_t$and h_b for the top and bottom faces, respectively, Young's modulus $E_i(i=t,b)$and Poisson's ratio $\nu_i(i=t,b)$, as depicted in Fig. 1f.

The first variation of the kinetic energy for the FGM sandwich plate with temperature dependent properties reads:

$$\int_{t_1}^{t_2}\delta T\,dt=-\int_{t_1}^{t_2}\Big\{\int_0^a\int_0^b\int_{-h_t/2}^{h_t/2}\rho_t(z_t,T_t)(\ddot{u}_t\delta u_t+\ddot{v}_t\delta v_t+\ddot{w}_t\delta w_t)\,dz_t dy dx+\int_0^a\int_0^b\int_{-h_b/2}^{h_b/2}\rho_b(z_b,T_b)(\ddot{u}_b\delta u_b+\ddot{v}_b\delta v_b+\ddot{w}_b\delta w_b)\,dz_b dy dx+\int_0^a\int_0^b\int_{-h_c/2}^{h_c/2}\rho_c(T_c)(\ddot{u}_c\delta u_c+\ddot{v}_c\delta v_c+\ddot{w}_c\delta w_c)\,dz_c dy dx\Big\}\,dt \qquad (2)$$

Where z_t, z_b and z_c are the vertical coordinates of the top and bottom face sheets and the core, respectively, and are measured downward from the mid-plane of each them; u_i , v_i and $w_i (i = t, b, c)$ are the displacements in the x , y and vertical directions, respectively, of the sandwich plate constituents (see Fig. 1f); $\ddot{u}_i$, $\ddot{v}_i$ and $\ddot{w}_i (i = t, b, c)$are the accelerations in the x , y and vertical directions, respectively, of the sandwich plate constituents; Subscripts t, b and c correspond to the upper face sheet, lower face sheet and the core, respectively;T_t, T_b and T_c are the temperature variation of the top and bottom face sheets and the core, respectively; $\rho_t(z_t, T_t)$ and $\rho_b(z_b, T_b)$ are the density of the upper and lower FGM face sheets, respectively, that varies in the thickness with z_t and z_b by power low function of FGMs (see Appendix A) and varies with temperature variation in each them, too; and $\rho_c(T_c)$ is the density of the core that varies with temperature in it.

The material properties of both faces and the core P, such as Young's modulus, density, thermal expansion coefficient and even Poisson's ratio, can be expressed as a nonlinear third-order function of temperature as [46]

$$P = C_0(C_{-1}T^{-1} + 1 + C_1T + C_2T^2 + C_3T^3) \tag{2.5}$$

Where C_0, C_{-1}, C_1, C_2 and C_3 are unique to the constituent materials; and $T = T_0 + \Delta T$ that $T_0 = 300K$ is the temperature.

Considering small deformations and rotations, the kinematic relations for the faces, based on Bernoulli assumptions, are

$$u_j(x, y, z_j, t) = u_{0j}(x, y, t) - z_j w_{j,x}(x, y, t) \tag{3}$$

$$v_j(x, y, z_j, t) = v_{0j}(x, y, t) - z_j w_{j,y}(x, y, t), (j = t, b) \tag{4}$$

$$w_j(x, y, z_j, t) = w_j(x, y, t) \tag{5}$$

Where $u_{0j}(x, y, t)$and $v_{0j}(x, y, t), (j = t, b)$ are the in-plane deformations of the mid-plane of each face sheet in the x and y directions, respectively; and $w_j(x, y, t)$, $(j = t, b)$ are the transverse deflections of each face sheet (see Fig. 1f).

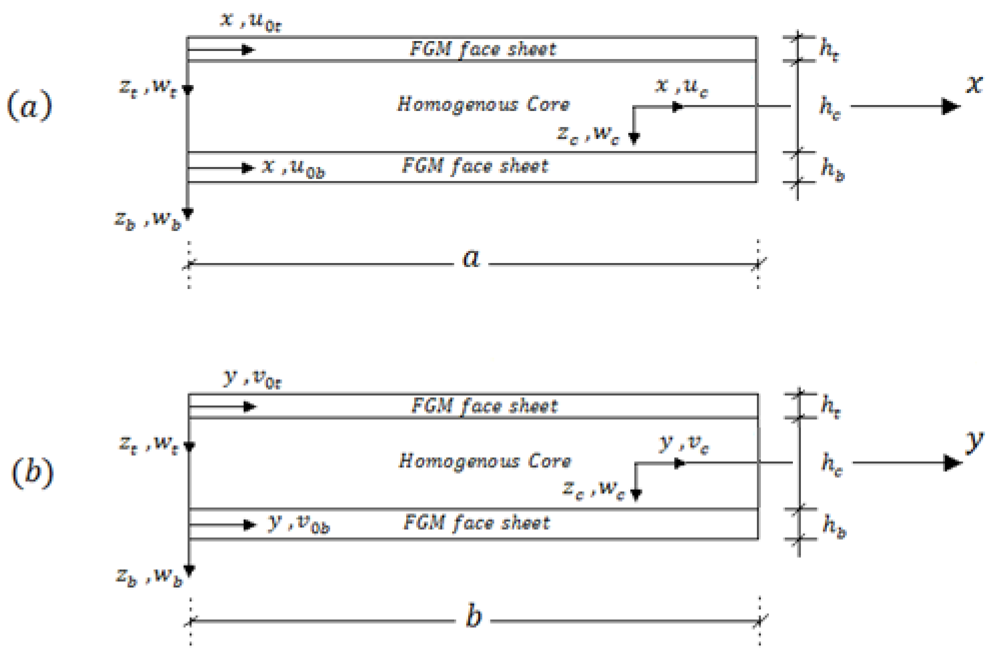

Fig.1. Geometry of FGM sandwich plate: (a) Geometry of x-z plane view; (b) Geometry of y-z plane view.

In this model, the displacement fields of the core are assumed a priori, using the quadratic and cubic polynomial distributions [45]. Here, the coefficients of these polynomials are the unknowns, and they are determined through the variational principle.

The pre-assumed displacement fields of the core read:

$$u_c(x,y,z_c,t) = u_0(x,y,t) + u_1(x,y,t)z_c + u_2(x,y,t){z_c}^2 + u_3(x,y,t){z_c}^3 \quad (6)$$

$$v_c(x,y,z_c,t) = v_0(x,y,t) + v_1(x,y,t)z_c + v_2(x,y,t){z_c}^2 + v_3(x,y,t){z_c}^3 \quad (7)$$

$$w_c(x,y,z_c,t) = w_0(x,y,t) + w_1(x,y,t)z_c + w_2(x,y,t){z_c}^2 \quad (8)$$

Where u_k and $v_k (k = 0,1,2,3)$ are the unknowns of the in-plane displacements of the core, and $w_l (l = 0,1,2)$ are the unknowns of the core vertical displacements.

The compatibility conditions, assuming perfect bonding between the core and the face sheets, at the upper and the lower face–core interfaces, $(z_c = 0, h_c)$, read

$$u_t(z_t = h_t/2) = u_c(z_c = -h_c/2) \quad (9)$$

$$v_t(z_t = h_t/2) = v_c(z_c = -h_c/2) \quad (10)$$

$$w_t = w_c(z_c = -h_c/2) \quad (11)$$

$$u_c(z_c = h_c/2) = u_b(z_b = -h_b/2) \quad (12)$$

$$v_c(z_c = h_c/2) = v_b(z_b = -h_b/2) \quad (13)$$

$$w_c(z_c = h_c/2) = w_b \quad (14)$$

The compatibility conditions at the upper and the lower face–core interfaces, Eqs. (9-e14), are enforced through the use of six Lagrange multipliers. Thus the first variation of the internal potential energy reads:

$$\delta U = \int_{V_t} \left(\sigma_{xx}^t \delta\varepsilon_{xx}^t + \sigma_{yy}^t \delta\varepsilon_{yy}^t + \tau_{xy}^t \delta\gamma_{xy}^t\right) dV + \int_{V_b} \left(\sigma_{xx}^b \delta\varepsilon_{xx}^b + \sigma_{yy}^b \delta\varepsilon_{yy}^b + \tau_{xy}^b \delta\gamma_{xy}^b\right) dV + \int_{V_{core}} \left(\tau_{xz}^c \delta\gamma_{xz}^c + \tau_{yz}^c \delta\gamma_{yz}^c + \sigma_{zz}^c \delta\varepsilon_{zz}^c + \sigma_{xx}^c \delta\varepsilon_{xx}^c + \sigma_{yy}^c \delta\varepsilon_{yy}^c + \tau_{xy}^c \delta\gamma_{xy}^c\right) dV + \delta \int_0^a \int_0^b \left[\lambda_{xt}\left(u_t(z_t = h_t/2) - u_c(z_c = -h_c/2)\right) + \lambda_{yt}\left(v_t(z_t = h_t/2) - v_c(z_c = -h_c/2)\right) + \lambda_{zt}\left(w_t - w_c(z_c = -h_c/2)\right) + \lambda_{xb}\left(u_c(z_c = h_c/2) - u_b(z_b = -h_b/2)\right) + \lambda_{yb}\left(v_c(z_c = h_c/2) - v_b(z_b = -h_b/2)\right) + \lambda_{zb}\left(w_c(z_c = h_c/2) - w_b\right)\right] dxdy \quad (15)$$

where σ_{xx}^j and σ_{yy}^j (j = t,b,c) are the in-plane stresses and ε_{xx}^j and ε_{yy}^j (j = t,b,c) are the in-plane strains of the upper and the lower face sheets and the core, $\tau_{xy}^j$and γ_{xy}^j (j = t,b,c) are the in-plane shear stresses and strains in faces and core; σ_{zz}^c and ε_{zz}^c are the normal stress and strain in the vertical direction of the core; τ_{xz}^c and γ_{xz}^c are the vertical shear stressand shear strain in the core; V_t, $V_b$and $V_{core}$are the volumes of the upper and lower face sheets and the core, respectively; λ_{xi} , λ_{yi} and λ_{zi} $(i = t, b)$ are the Lagrange multipliers at the upper and the lower face–core interfaces; and δ is the variation operator. Notice that the effects of core in-plane stresses are considered in this formulation.

The kinematic relations used, assuming small deformations, take the following form for the face sheets:

$$\varepsilon_{xx}^j(x,y,z_j,t) = u_{0j,x}(x,y,t) - z_j w_{j,xx}(x,y,t) \quad (16)$$

$$\varepsilon_{yy}^j(x,y,z_j,t) = v_{0j,y}(x,y,t) - z_j w_{j,yy}(x,y,t), (j = t,b) \quad (17)$$

$$\gamma_{xy}^j(x,y,z_j,t) = u_{0j,y}(x,y,t) + v_{0j,x}(x,y,t) - 2z_j w_{j,xy}(x,y,t) \quad (18)$$

Where $(\,)_{,i}$ denotes a partial derivative with respect to i. The kinematic relations for the core:

$$\varepsilon_{xx}^c = u_{0,x} + u_{1,x}z_c + u_{2,x}{z_c}^2 + u_{3,x}{z_c}^3 \quad (19)$$

$$\varepsilon_{yy}^c = v_{0,y} + v_{1,y}z_c + v_{2,y}{z_c}^2 + v_{3,y}{z_c}^3 \quad (20)$$

$$\varepsilon_{zz}^c = w_1 + 2w_2 z_c \quad (21)$$

$$\gamma_{xz}^c = \left(u_1 + w_{0,x}\right) + \left(2u_2 + w_{1,x}\right)z_c + \left(3u_3 + w_{2,x}\right){z_c}^2 \quad (22)$$

$$\gamma_{yz}^c = \left(v_1 + w_{0,y}\right) + \left(2v_2 + w_{1,y}\right)z_c + \left(3v_3 + w_{2,y}\right){z_c}^2 \quad (23)$$

$$\gamma_{xy}^c = \left(u_{0,y} + v_{0,x}\right) + \left(u_{1,y} + v_{1,x}\right)z_c + \left(u_{2,y} + v_{2,x}\right){z_c}^2 + \left(u_{3,y} + v_{3,x}\right){z_c}^3 \quad (24)$$

Using the Hamilton's principle, Eq. (1); the expression ofthe kinetic energy and internal potential energy, Eq. (2) and (15), along with the acceleration distribution,based on Eqs.(6-e8); the displacements distributions of the face sheets, Eqs.(3-e5); the kinematic relations of the faces andthe core, see Eqs. (16-e24); the compatibility conditions correspondingto perfect bonding at the face–core interfaces, Eqs. (9-e14); the stress resultants of the face sheets, Appendix A, andthe high-order stress resultants of the core, Appendix C. Hence, after some algebraic manipulation the twenty three equations of motionread:

Three equations for the top FGM face sheet:

$$N_{xx,x}^{t}+N_{xy,y}^{t}-\lambda_{xt}-I_{0t}\ddot{u}_{0t}+I_{1t}\ddot{w}_{t,x}=0 \quad (25)$$

$$N_{yy,y}^{t}+N_{xy,x}^{t}-\lambda_{yt}-I_{0t}\ddot{v}_{0t}+I_{1t}\ddot{w}_{t,y}=0 \quad (26)$$

$$M_{xx,xx}^{t}+M_{yy,yy}^{t}+2M_{xy,xy}^{t}-\frac{h_t}{2}\lambda_{xt,x}-\lambda_{zt}-\frac{h_t}{2}\lambda_{yt,y}-I_{1t}\ddot{u}_{0t,x}+I_{2t}\ddot{w}_{t,xx}-I_{1t}\ddot{v}_{0t,y}+I_{2t}\ddot{w}_{t,yy}-I_{0t}\ddot{w}_{t}=0 \quad (27)$$

Three equations for the bottom FGM face sheet:

$$N_{xx,x}^{b}+N_{xy,y}^{b}+\lambda_{xb}-I_{0b}\ddot{u}_{0b}+I_{1b}\ddot{w}_{b,x}=0 \quad (28)$$

$$N_{yy,y}^{b}+N_{xy,x}^{b}+\lambda_{yb}-I_{0b}\ddot{v}_{0b}+I_{1b}\ddot{w}_{b,y}=0 \quad (29)$$

$$M_{xx,xx}^{b}+M_{yy,yy}^{b}+2M_{xy,xy}^{b}-\frac{h_b}{2}\lambda_{xb,x}+\lambda_{zb}-\frac{h_b}{2}\lambda_{yb,y}-I_{1b}\ddot{u}_{0b,x}+I_{2b}\ddot{w}_{b,xx}-I_{1b}\ddot{v}_{0b,y}+I_{2b}\ddot{w}_{b,yy}-I_{0b}\ddot{w}_{b}=0$$

$$u_{0t}-\frac{h_t}{2}w_{t,x}-u_0+u_1\frac{h_c}{2}-u_2\frac{h_c^2}{4}+u_3\frac{h_c^3}{8}=0 \quad (42)$$

$$v_{0t}-\frac{h_t}{2}w_{t,y}-v_0+v_1\frac{h_c}{2}-v_2\frac{h_c^2}{4}+v_3\frac{h_c^3}{8}=0 \quad (43)$$

$$w_t-w_0+w_1\frac{h_c}{2}-w_2\frac{h_c^2}{4}=0 \quad (44)$$

$$u_0+u_1\frac{h_c}{2}+u_2\frac{h_c^2}{4}+u_3\frac{h_c^3}{8}-u_{0b}-\frac{h_b}{2}w_{b,x}=0 \quad (45)$$

$$v_0+v_1\frac{h_c}{2}+v_2\frac{h_c^2}{4}+v_3\frac{h_c^3}{8}-v_{0b}-\frac{h_b}{2}w_{b,y}=0 \quad (46)$$

$$w_0+w_1\frac{h_c}{2}+w_2\frac{h_c^2}{4}-w_b=0 \quad (47)$$

Where N_{xx}^{j} , N_{yy}^{j} , N_{xy}^{j} , M_{xx}^{j} , M_{yy}^{j}, M_{xy}^{j} $(j=t,b)$ are the stress resultants and the moment resultants of the upper and lower face sheets (see Appendix A); I_{kt} , I_{kb} $(k=0,1,2)$ are the inertia terms of the top and bottom face sheets, respectively (see Appendix B); I_{lc} $(l=0,1,2,3,4,5,6)$ are the inertia terms of the core (see Appendix B).

Where, all stress components of the core are temperature dependent, see Appendix C. Thus, the number of equations including the compatibility equations is twenty three. The set of governing equations consists of six equilibrium equations for the face sheets, Eqs. (25-e30), eleven equations for the core, Eqs.(31-e41), and six compatibility equations, Eqs.(42-e47).

In order to determine the governing equations of motion the high-order stress resultant terms of the core must be defined first in terms of the displacements. The stress fields and the high-order terms are derived assuming that the core is isotropic, using the pre-assumed displacements patterns, Eqs. (6-e8), and the high-order terms, Eqs.(48-e53). Hence, the core stresses and the core stress resultants are expressed in Appendix C for the sake of brevity.

Finally, the governing equations of motion are derived by substituting the stress resultants of the face sheets, Appendix C, into the governing equations for the face sheets, Eqs. (25-e30), and the high-order stress resultants of the core into the core equations, Eqs.(31-e41). These equations are formulated in terms of the following twenty three unknowns: the in-plane and vertical displacements of the face sheets, the six Lagrange multipliers and the eleven polynomial coefficients of the core. Notice that the solution of the set equations can be achieved numerically for general type of boundary conditions but does not have a general closed-form analytical solution. However, for the particular case of a simply-supported sandwich plate a closed-form solution exists.

3. Simply supported plate

An analytical solution exists in the case of a simply supported sandwich plate where the upper and the lower face sheets are simply supported and the vertical displacements through the depth of the core at the edges of the plate are prevented. Furthermore, the face sheets are assumed to be functionally graded and the core is assumed to be isotropic. For this case an analytical closed-form solution in the form of an infinite series of trigonometric functions, which satisfies the boundary conditions exist. The solution can be expressed as:

$$u_{0j}(x,y,t) = \left[\sum_{n=1}^{N}\sum_{m=1}^{M} C_{uj} cos(\alpha_m x) sin(\beta_n y)\right] e^{I\omega t}, \quad (j = t, b) \tag{54}$$

$$v_{0j}(x,y,t) = \left[\sum_{n=1}^{N}\sum_{m=1}^{M} C_{vj} sin(\alpha_m x) cos(\beta_n y)\right] e^{I\omega t}, \quad (j = t, b) \tag{55}$$

$$w_j(x,y,t) = \left[\sum_{n=1}^{N}\sum_{m=1}^{M} C_{wj} sin(\alpha_m x) sin(\beta_n y)\right] e^{I\omega t}, \quad (j = t, b) \tag{56}$$

$$u_k(x,y,t) = [\sum_{n=1}^{N}\sum_{m=1}^{M} C_{uk} cos(\alpha_m x) sin(\beta_n y)] e^{I\omega t}, \quad (k = 0,1,2,3) \tag{57}$$

$$v_k(x,y,t) = [\sum_{n=1}^{N}\sum_{m=1}^{M} C_{vk} sin(\alpha_m x) cos(\beta_n y)] e^{I\omega t}, \quad (k = 0,1,2,3) \tag{58}$$

$$w_l(x,y,t) = [\sum_{n=1}^{N}\sum_{m=1}^{M} C_{wl} sin(\alpha_m x) sin(\beta_n y)] e^{I\omega t}, \quad (l = 0,1,2) \tag{59}$$

WhereC_{uj} , C_{vj} , C_{wj} , C_{uk} , C_{vk}, C_{wl} , $C_{\lambda xj}$, $C_{\lambda yj}$and $C_{\lambda zj}$ are the twenty three unknown constants of the series solution, in the other words C_{uj} , C_{vj} and C_{wj} are the six face sheets constants, $C_{\lambda xj}$, $C_{\lambda yj}$and $C_{\lambda zj}$ are the six Lagrange constants, and C_{uk} , C_{vk} and C_{wl} are the eleven core constants; $\alpha_m = \frac{m\pi}{a}$ and $\beta_n = \frac{n\pi}{b}$ where m and n are the wave numbers; M and N are the number of terms in the truncated series; ω is the eigenfrequency of the plate; and I is the imaginary unit.

After substitution of a general term of the series, see Eqs. (54-e62), into the equations of motion, see Eqs. (25–e47), along with the stress resultants of functionally graded face sheets, see Appendix A, and the high-order stress resultants of the core, see Appendix C, the solution is determined by use a new approach to solve these twenty three equations of motion.

The new solution approach consists of isolating six unknown constants of the face sheets as a function of eleven core constants using the six compatibility equations, Eqs. (42-e47), followed by isolating the additional six Lagrange constants as a function of face sheets constants using the six equations of the face sheets, Eqs. (25-e30). Then, the isolated unknown constants are substituted into the eleven equations of the core, Eqs. (31-e41). Finally, we have eleven equations just functions of eleven core constants. This approach illustrated clearly in Fig. 2f.

Thus, although the full set of the governing equations consist of twenty three equations, see Eqs. (25)–(47), the actual number of eigenfrequencies is only eleven. And so, the mass and the stiffness matrices are dimension eleven. This yields a set of homogeneous algebraic equations for each wave numbers m and n that may be described by a mass and a stiffness matrix, where the eigenfrequency equals to the eigenvalue and the series constants for each wave numbers m and n are the corresponding eigenvectors as follows:

$$(\boldsymbol{K_{mn}} - \omega_{mn}^2 \boldsymbol{M_{mn}})\boldsymbol{C_{mn}} = \boldsymbol{0} \tag{63}$$

Where $\boldsymbol{K}_{mn}$ and $\boldsymbol{M}_{mn}$ are the stiffness and the mass matrices that correspond to the m'th and n'th harmonic term in the series and are not presented for the sake of brevity; ω_{mn} is the eigenfrequency that corresponds to the m'th and n'th term; $\mathbf{0}$ is a null vector; and $\boldsymbol{C}_{mn}$ is the eigenvector that its components are equal to eleven core constants:

$$\boldsymbol{C}_{mn} = [C_{u0} C_{u1} C_{u2} C_{u3} C_{v0} C_{v1} C_{v2} C_{v3} C_{w0} C_{w1} C_{w2}] \tag{64}$$

4. Verification

The numerical results of rectangular simply supported sandwich plates with power-law FGM face sheets are verified in this section.

Considering an FGM sandwich plate as shown in Fig. 3f, the Young's modulus and mass density of bottom face sheet at $z = h_c/2$ and top face sheet at $z = -h_c/2$ are 380Gpaand $3800\,kg/m^3$, respectively (the properties of alumina). In the bottom face sheet at $z = (h_c/2 + h_b)$ and in the top face sheet at $z = -(h_c/2 + h_t)$ the Young's modulus and mass density are 70Gpaand $2707\,kg/m^3$, respectively (the properties of aluminum). And the Young's modulus and mass density in each face sheet vary according to the power-law function. Poisson's ratio is equal to 0.3 throughout the analyses. For simplicity, the non-dimensional natural frequency parameter is defined as [47]

$$\varpi = \frac{\omega b^2}{h_b + h_c + h_t}\sqrt{\frac{\rho_0}{E_0}} \quad , \quad (\rho_0 = 1\,kg/m^3 \,, E_0 = 1Gpa) \tag{65}$$

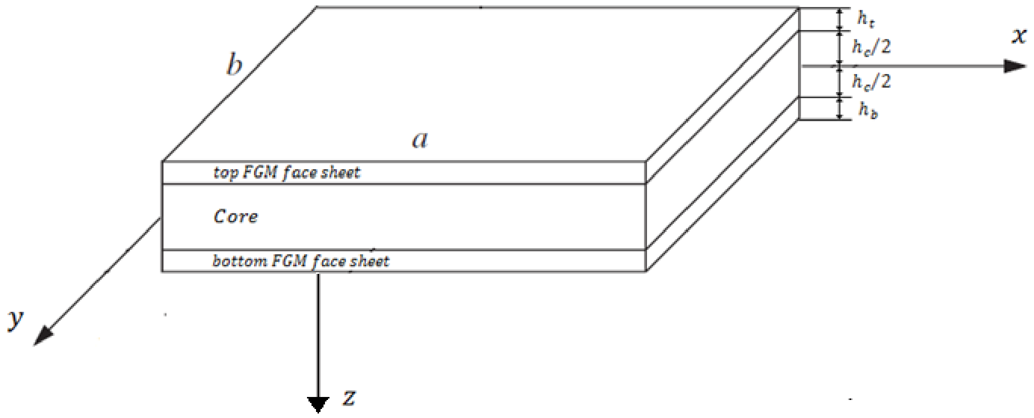

Fig. 3f. Geometry of simply supported sandwich plate with FGM face sheets

Table 1t shows the comparison of flexural vibration frequency parameter ϖ of present study and [47] for square 2-1-2 sandwich plates with power-law functionally graded face sheets and homogeneous hard core with volume fraction index κ values ($\kappa = 1,10$) and two thickness ratios ($h/b = 0.01, 0.1$). Where 2-1-2 sandwich plate is an symmetric sandwich that the face sheet thickness is two times of core thickness.

Table 1t: Comparisons of flexural vibration frequency parameters ϖ of present study for 2-1-2 sandwich FGM plate with [47], ($\frac{a}{b} = 1$)

	κ=1		κ=10	
h/b	*[47]*	*present*	*[47]*	*present*
0.01	1.32974	1.32748	0.95937	1.00676
0.1	1.30186	1.31011	0.94283	0.99656

The results of simply supported square sandwich plates with functionally graded faces and homogeneous hard core are compared in Table 2t with the results from [47] for five different face and core thicknesses. Young's modulus and mass density in the faces are based on the power-law distribution, see Appendix A. Table 2t shows a good agreement by comparisons of FGM sandwich plates of four different volume fraction indices κ=0.5,1,5,10 with [47].

Table 2t: verifying of natural fundamental frequency parameters $\overline{\omega}$ of square hard core sandwich plates with FGM faces, ($\frac{h}{b} = 0.1$)

	2-1-2		*2-1-1*		*1-1-1*		*2-2-1*		*1-2-1*	
κ	*[47]*	*present*	*[47]*	*present*	*[47]*	*present*	*[47]*	*present*	*[47]*	*present*
0.5	1.48608	1.45617	1.50841	1.47199	1.52131	1.49097	1.54926	1.50896	1.57668	1.53528
1	1.30181	1.31011	1.33511	1.33479	1.35523	1.35165	1.39763	1.38092	1.44137	1.41319
5	0.98103	1.05333	1.02942	1.08934	1.04532	1.08652	1.10983	1.13234	1.17567	1.16613
10	0.94078	0.99656	0.98929	1.03426	0.99523	1.02398	1.06104	1.07273	1.12466	1.10578

The two types of square power-law FGM sandwich plates with homogeneous soft core and homogeneous hard core are investigated. Four-layer thickness ratios (2-1-2, 1-1-1, 2-2-1, 1-2-1) are selected for the comparison with [47]. Tables 3t and 4t give the fundamental frequency parameters $\overline{\omega}$ of these selected plates, that are verified with similar results of [47].

Tables 3t consider the case of homogeneous hard core in which the Young's modulus and mass density at $z = \pm h_c/2$ are 380 Gpaand $3800\,kg/m^3$, respectively, and at $z = -(h_c/2 + h_t)$ and $z = (h_c/2 + h_b)$ are 70 Gpa and $2707\,kg/m^3$, respectively. Tables 4t consider the case of homogeneous soft core in which the Young's modulus and mass density at $z = \pm h_c/2$ are 70 Gpaand $2707\,kg/m^3$, respectively, and at $z = -(h_c/2 + h_t)$ and $z = (h_c/2 + h_b)$ are 380 Gpa and $3800\,kg/m^3$, respectively. Thickness-side ratio is $h/b = 0.01$ and three volume fraction indices κ (1,5,10) are considered. Tables 3t and 4t indicate the results of fundamental frequency calculated with present analysis are in good agreement with results of [47].

Table 3t: Comparison of fundamental frequency parameters $\overline{\omega}$ with [47], for square hard core sandwich plates, ($\frac{h}{b} = 0.01$)

	2-1-2		*1-1-1*		*2-2-1*		*1-2-1*	
κ	*[47]*	*present*	*[47]*	*present*	*[47]*	*present*	*[47]*	*present*
1	1.32974	1.32748	1.38511	1.37485	1.42992	1.40626	1.47558	1.44351
5	0.99903	1.06465	1.06309	1.10095	1.13020	1.14883	1.19699	1.18585
10	0.95934	1.00676	1.01237	1.03671	1.08065	1.08746	1.14408	1.12336

Table 4t: Comparison of fundamental frequency parameters $\overline{\omega}$ with [47], for square soft core sandwich plates, ($\frac{h}{b} = 0.01$)

	2-1-2		*1-1-1*		*2-2-1*		*1-2-1*	
κ	*[47]*	*present*	*[47]*	*present*	*[47]*	*present*	*[47]*	*present*
1	1.79163	1.79185	1.75379	1.75252	1.68184	1.67323	1.67490	1.66900
5	1.94313	1.91014	1.93623	1.90684	1.86207	1.83289	1.88530	1.85992
10	1.94687	1.92450	1.95044	1.92970	1.88042	1.85849	1.91162	1.89235

4. Numerical results

Square sandwich plate with side-to-thickness ratio $a/h = 10$ is considered. Note that the core of the plate is fully Stainless Steel while the top and bottom face sheets of the plate are Silicon Nitride/Stainless Steel functionally graded materials and properties distribution in thickness of the face sheets is by Power-law function, see Fig. 4f. Table 5t shows the Temperature dependent properties of constituent materials of the FGM face sheets [46]. Fig. 5f, 6f and 7f depict the fundamental frequency parameters ϖ versus temperatures of 1-8-1, 1-1-1 and 2-1-2 simply supported FGM sandwich plates, respectively, for five values of power-law index ($\kappa = 0, 0.2, 1, 5, \infty$).

It is seen that the fundamental frequency parameters ϖ increase with increases the face sheet thickness than core thickness in 1-8-1(Fig. 5f), 1-1-1(Fig. 6f) and 2-1-2(Fig. 7f) FGM sandwich plates, respectively. Because the amount of ceramic and so structural stiffness increase with increases the face sheet thickness. It is also shown in Fig. 5f, 6f and 7f that for lower temperatures and for higher power-law indices, the amounts of fundamental frequency parameters are bigger as expected.

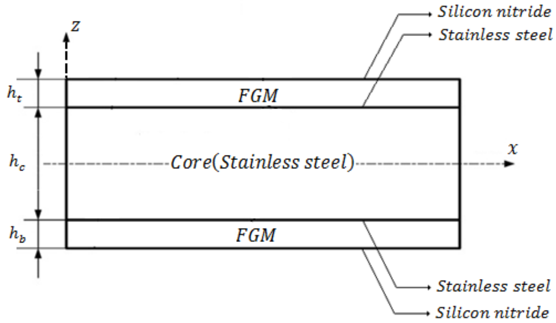

Fig. 4f: Tow dimensional view of simply supported sandwich plate with (Silicon Nitride/Stainless Steel) FGM faces and Stainless Steel core.

Table 5t:Temperature dependent properties of constituent materials of the FGM face sheets [46]

	Silicon nitride(Si_3N_4)			Stainless steel($SUS304$)		
	E	ν	ρ	E	ν	ρ
C_0	348.4323×10^9	0.24	2370	201.03547×10^9	0.32622351	8166
C_{-1}	0	0	0	0	0	0
C_1	$-3.0697386 \times 10^{-4}$	0	0	3.079296×10^{-4}	-2.001822×10^{-4}	0
C_2	2.160186×10^{-7}	0	0	-6.533871×10^{-7}	3.7973578×10^{-7}	0
C_3	$-8.946165 \times 10^{-11}$	0	0	0	0	0

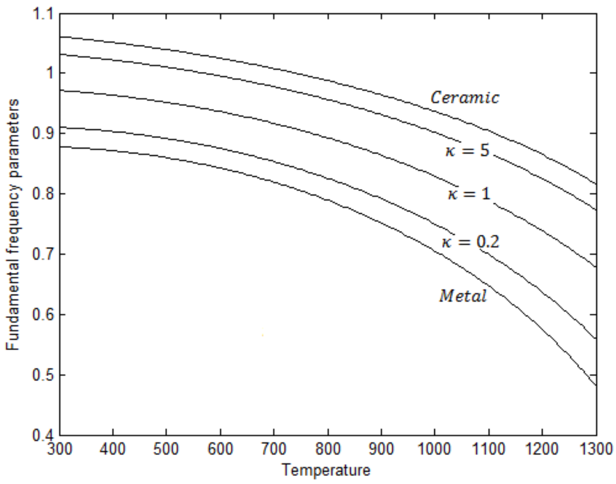

Fig. 5f. Variation of fundamental frequency parameter ϖ with temperature, for 1-8-1 and (Silicon Nitride/Stainless Steel/ Silicon Nitride) FGM sandwich plates at different power-law indices κ. $(a/b = 1, a/h = 10)$

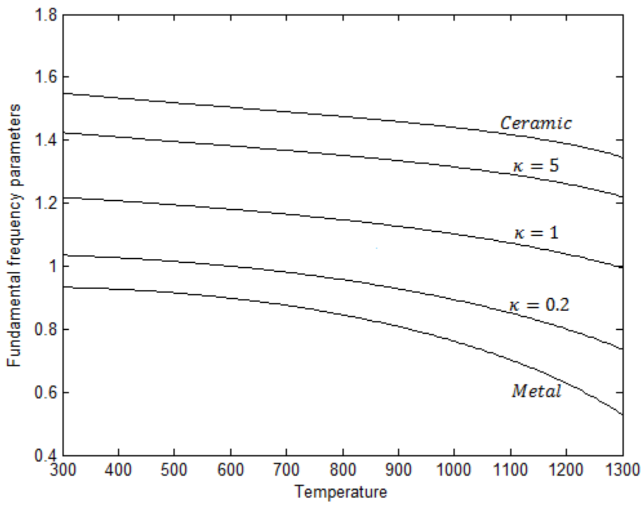

Fig. 6f. Variation of fundamental frequency parameter $\overline{\omega}$ with temperature, for 1-1-1 and (Silicon Nitride/Stainless Steel/ Silicon Nitride) FGM sandwich plates at different power-law indices κ. $(a/b = 1, a/h = 10)$

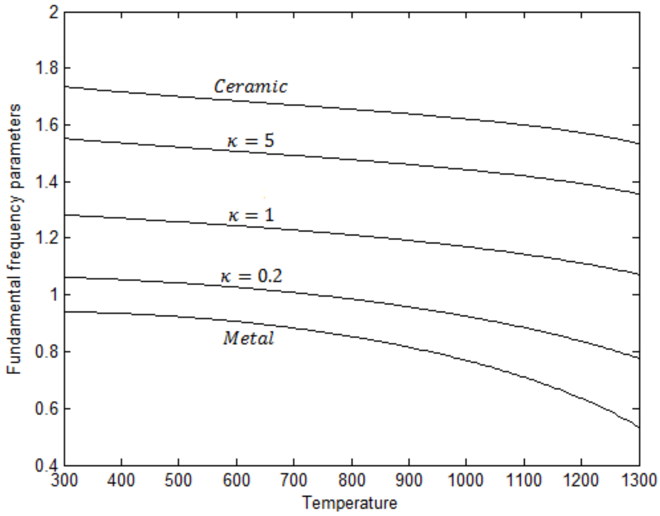

Fig. 7f. Variation of fundamental frequency parameter $\overline{\omega}$ with temperature, for 2-1-2 and (Silicon Nitride/Stainless Steel/ Silicon Nitride) FGM sandwich plates at different power-law indices κ. $(a/b = 1, a/h = 10)$

Figs. 8f, 9f and 10f display the fundamental frequency parameters in different temperatures versus power-law index for 1-8-1, 1-1-1 and 2-1-2 FGM sandwich plates, respectively. It is shown that the effect of temperature on the value of fundamental frequency parameters decrease with increases the FGM face sheets thickness. Because, the effect of temperature on the metal properties is more important than the effect of temperature on the ceramic properties.

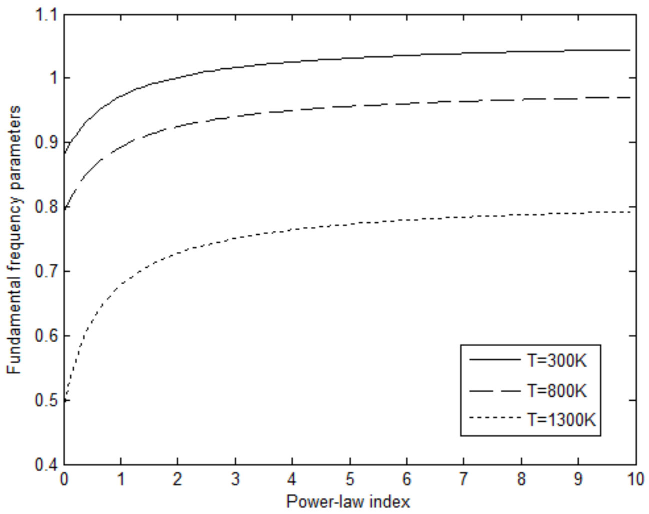

Fig. 8f. Variation of fundamental frequency parameter $\bar{\omega}$ with power-law index κ, for 1-8-1 and (Silicon Nitride/Stainless Steel/ Silicon Nitride) FGM sandwich plates at different temperatures. $(a/b = 1, a/h = 10)$

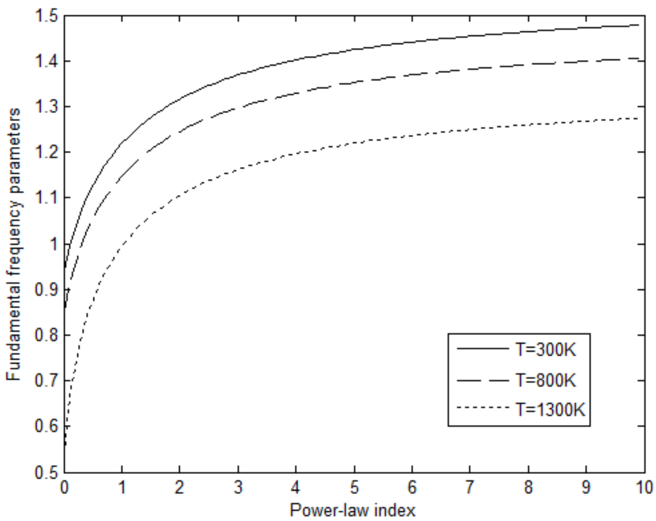

Fig. 9f. Variation of fundamental frequency parameter $\bar{\omega}$ with power-law index κ, for 1-1-1 and (Silicon Nitride/Stainless Steel/ Silicon Nitride) FGM sandwich plates at different temperatures. $(a/b = 1, a/h = 10)$

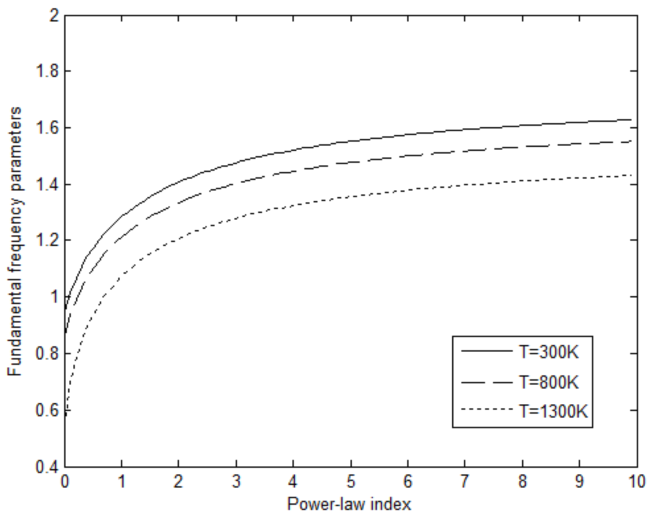

Fig. 10f. Variation of fundamental frequency parameter $\bar{\omega}$ with power-law index κ, for 2-1-2 and (Silicon Nitride/Stainless Steel/ Silicon Nitride) FGM sandwich plates at different temperatures. $(a/b = 1, a/h = 10)$

The fundamental frequency parameters $(\bar{\omega})$ versus side-to-thickness ratio (b/h) for square sandwich plates are plotted in Figs. 11f, 12f and 13f. These figures are plotted for 1-8-1, 1-1-1, and 2-1-2 sandwiches and for different temperatures and power law indices. In this figures, the fundamental frequency parameters increase with increasing the side-to-thickness ratio. It should be notice that for side-to-thickness ratio greater than about ten $(b/h > 10)$, the variation of fundamental frequency parameters are very small. This result indicates that $\bar{\omega}$ is almost constant for high aspect ratio FGM sandwich plates. Furthermore, increase in the face sheet thickness, decrease in temperature, and increase in the power law index are cause to increase in the fundamental frequency parameters.

Figs. 14f and 15f show the Fundamental frequency parameters for various core-to-face sheet thickness ratios. Results related to different temperatures and different power law indices are shown in Figs. 14f and 15f, respectively. From these two Figures, it is observed that the Fundamental frequency parameters decrease with increasing the core-to-face sheet thickness ratios. This is due to the fact that core is softer than face sheets. This Result was reverse if we had a hard core sandwich plate. From Figs. 14f and 15f, one could also observe that the Fundamental frequency parameters increase with increasing the power law index and decreasing the temperature, as expected.

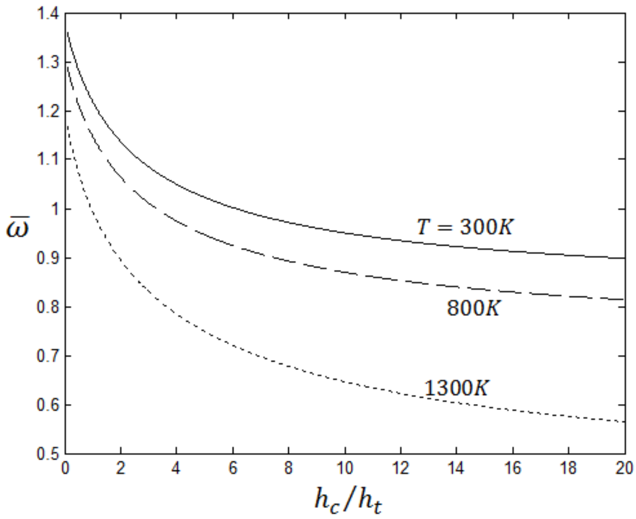

Fig. 14f. Fundamental frequency parameters $(\bar{\omega})$ as a function of h_c/h_t, for (Silicon Nitride/Stainless Steel/ Silicon Nitride) FGM symmetric sandwich plates at different temperatures. $(a/b = 1, a/h = 10, \kappa = 1)$

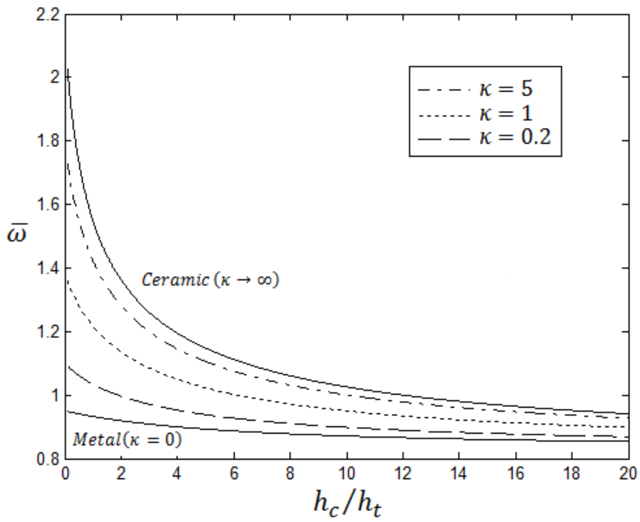

Fig. 15f. Fundamental frequency parameters ($\overline{\omega}$) as a function of h_c/h_t, for (Silicon Nitride/Stainless Steel/ Silicon Nitride) FGM symmetrical sandwich plates at different power-law index κ.$(\mathrm{a/b} = 1, \mathrm{a/h} = 10, T = 300K)$

7. Conclusions

An improved high-order sandwich plate theory is used to analyze the free vibration of sandwich plates with FGM face sheets and temperature dependent properties. The second model of Frostig that assumes the through-the thickness displacements distributions of the core are quadratic and cubic for the vertical and horizontal displacements and accelerations, respectively, is used in present paper. Hence, the unknowns in this model consist of the coefficients of these polynomial together with the face sheet displacements. This model implicates the existence of higher-order stress resultants in the core, which cannot be associated with any meaningful physical interpretation. This model is improved by considering the in-plane stresses of the core and equations of motion are solved by use a new approach.

References

[1] Hui-ShenShen, Shi-Rong Li. Postbuckling of sandwich plates with FGM face sheets and temperature-dependent properties. Composites: Part B 39 (2008) 332–344..
[2] .stress in sandwich plate with functionally graded coatings. Thin Solid Films 516 (2008) 7581–7587.
[3] H.G. Allen, Analysis and Design of Structural Sandwich Panels, Pergamon Press, London, 1969.
[4] F.J. Plantema, Sandwich Construction, Wiley, New York, 1966.
[5] D. Zenkert, An Introduction to Sandwich Construction, Chameleon Press Ltd., London, 1995.
[6] J.R. Vinson, The Behavior of Sandwich Structures of Isotropic and Composite Materials, Technomic Publishing Co. Inc, Lancaster, 1999.
[7] A.K. Noor, W.S. Burton, C.W. Bert, Computational models for sandwich panels and shells, Appl. Mech. Rev. 49 (1996) 155–199.] L. Librescu, T. Hause, Recent developments in the modeling and behavior of advanced sandwich constructions: a survey, Compos. Struct. 48 (1) (2000) 1–17.
[8] R.D. Mindlin, Influence of transverse shear deformation on the bending of classical plates, Trans. ASME, J. Appl. Mech. 8 (1951) 18–31.
[9] J.N. Reddy, Energy and Variational Methods in Applied Mechanics, Wiley, New York, 1984.
[10] Carrera E, Demasi L. Two benchmarks to assess two-dimensional theories of sandwich, composite plates. AIAA J 2003;41(7):1356–62.
[11] Carrera E, Ciuffreda A. Bending of composites and sandwich plates subjected to localized lateral loadings: a comparison of various theories. Compos Struct 2005;68:185–202.
[12] Carrera E. Transverse normal strain effects on thermal stress analysis of homogeneous and layered plates. AIAA J 2005;43(10):2232–42.
[13] Kant T, Mallikarjuna. A high-order theory for free vibration of unsymmetrically laminated composite and sandwich plates – finite element evaluation. ComputStruct 1989;32(5):1125–32.
[14] Kant T, Swaminathan K. Analytical solution for free vibrations for laminated composite and sandwich plates based on a higher-order refined theory. Compos Struct 2001;53:73–85.
[15]Meunier M, Shenoi RA. Dynamic analysis of composite sandwich plates with damping modelled using high-order shear deformation theory. Compos Struct 2001;54:243–54.
[16]Bardell NS, Dundson JM, Langley RS. Free vibration analysis of coplanar sandwich panels. Compos Struct 1997;38(1-4):463–75.
[17] Lee LJ, Fan YJ. Bending and vibration analysis of composite sandwich plates. ComputStruct 1996;60(1):103–12.
[18]Vangipuram P, Ganesan N. Buckling and vibration of rectangular composite viscoelastic sandwich plates under thermal loads. Compos Struct 2007;77: 419–29.
[19]Shiau L-C, Kuo S-Y. Free vibration of thermally buckled composite sandwich plates. J VibratAcoust, ASME 2006;128:1–7.
[20] Ibrahim HH, Tawfik M, Al-Ajmi M. Aero-thermo-mechanical characteristic of functionally graded material with temperature-depenednt material properties. In: Proceeding of ICFDP 8: eight international congress of fluid dynamics and propulsion, December 14–17, 2006, Sharm El-Sheikh, Sinai, Egypt; 2006.
[21] Kim Y-W. Temperature dependent vibration analysis of functionally graded rectangular plates. J Sound Vibrat 2005;284:531–49.
[22]Hao M, Rao MD. Vibration and damping analysis of sandwich beam containing a viscoelastic constraining core. J Compos Mater 2005;39:1621–43.
[23]Duan B, Tawfik M, Goek S, Ro J, Mei C. Vibration of laminated composite plates embedded with shape memory

alloy at elevated temperatures. In: SPIE's 7th international symposium on smart structures and materials, vol. 3991, Newport Beach (CA, USA); March 2000.
[24] A. Petras, M.P.F. Sutcliffe. Indentation resistance of sandwich beams. J Compo Struct 1999; 46: 413-424.
[25] Y. Frostig, M. Baruch, O. Vilnay, I. Sheinman, A high order theory for the bending of sandwich beams with a flexible core, J. ASCE EM Division 118 (5) (1992) 1026–1043.
[26]Frostig Y, Baruch M. Localized load effects in high-order bending of sandwich panels with flexible core. J EngrgMech 1996;122(11):1069-1076.
[27] Y. Frostig, M. Baruch, Buckling of simply-supported sandwich beams with transversely flexible core—a high order theory, J. ASCE EM Division 119 (3) (1993) 476–495.
[28] Y. Frostig, Buckling of sandwich panels with a transversely flexible core—high-order theory, Int. J. Solids Struct. 35 (3–4) (1998) 183–204.
[29] V. Sokolinsky, Y. Frostig, Effects of boundary conditions in high-order buckling of sandwich panels with a transversely flexible core, J. ASCE EM Division 125 (8) (1999) 865–874.
[30] V. Sokolinsky, Y. Frostig, Non-linear behavior of sandwich panels with a transversely flexible core—high-order theory approach, AIAA J. 37 (11) (1999) 1474–1482.
[31] V. Sokolinsky,Y. Frostig, Branching behavior in the non-linear response of sandwich panels with a transversely flexible core, Int. J. Solids Struct. 37 (2000) 5745–5772.
[32]Frostig Y, Baruch M. Free vibration of sandwich beams with a transversely flexible core: a high order approach. J Sound Vibrat 1994;176(2):195–208.
[33]Bozhevolnaya E, Frostig Y. Free vibration of curved sandwich beams with a transversely flexible core. J Sandwich Struct Mater 2001;3(4):311–42.
[34]Frostig Y, Thomsen OT. High-order free vibration of sandwich panels with a flexible core. Int J Solids Struct 2004;41(5-6):1697–724.
[35] Yang MJ, Qiao P. Higher-order impact modeling of sandwich beams with flexible core. Int J Solids Struct 2005;42(20):5460–90.
[36]Qiao P, Yang MJ. Impact analysis of fiber reinforced polymer honeycomb composite sandwich beams'. Compos Part B: Eng 2007;38:739–50.
[37]Schwarts-Givli H, Rabinovitch O, Frostig Y. High order nonlinear contact effects in cyclic loading of delaminated sandwich panels. Compos Part B – Eng 2007;38(1):86–101.
[38]Schwarts-Givli H, Rabinovitch O, Frostig Y. High order nonlinear contact effects in the dynamic behavior of delaminated sandwich panels with flexible core. Int J Solids Struct 2007;44(1):77–99.
[39]Schwarts-Givli H, Rabinovitch O, Frostig Y. Free vibrations of delaminated unidirectional sandwich panels with a transversely flexible core – a modified Galerkin approach. J Sound Vibrat 2007;301(1–2):253–77.
[40]Schwarts-Givli H, Rabinovitch O, Frostig Y. Free vibration of delaminated sandwich panels with a transversely flexible core and general boundary conditions– a high order approach. J Sandwich Struct Mater 2008;10(2): 99–131.
[41]Malekzadeh K, Khalili MR, Mittal RK. Local and global damped vibrations of sandwich plates with a viscoelastic soft flexible core: an improved high-order approach. J Sandwich Struct Mater 2005;7(5):431–56.
[42]Frostig Y, Thomsen OT. Non-linear thermal response of sandwich panels with a flexible core and temperature dependent mechanical properties. Compos Part B: Eng 2008;39(1):165–84 [special issue, Rajapakse YDS.ON].
[43]Frostig Y, Thomsen OT. Buckling and non-linear response of sandwich panels with a compliant core and temperature-dependent mechanical properties. J Mech Mater Struct 2007;2(7).
[44] Y. Frostig ,O.T. Thomsen. On the free vibration of sandwich plates with a transversely flexible and temperature-dependent core material – part I: Mathematical formulation. J Composites Science and Technology 2008; ():-.
[45] J. N. Reddy, Thermo mechanical behavior of functionally graded materials.Texas,1998.
[46] Q. Li, V.P. Iu, K.P. Kou, Three-dimensional vibration analysis of functionally graded material sandwich plates, Journal of solid and vibration, 311 (2008) 498-515.
[47]Shyang-Ho Chi, Yen-Ling Chung. Mechanical behavior of functionally graded material plates under transverse load—Part I: Analysis. J Solids and Struct 2006; 43: 3657-3674.